

05,07

Chiral Hall effect during the first-order phase transition in ferromagnetic lanthanum manganites

© A.A. Povzner, A.N. Filanovich, E.I. Lopatko, N.A. Zaitceva

Ural Federal University named after the first President of Russia B.N. Yeltsin,
Yekaterinburg, Russia

E-mail: a.a.povzner@urfu.ru

Received July 9, 2025

Revised August 11, 2025

Accepted August 14, 2025

Based on the results of *ab initio* electronic structure modeling, the phase separation during magnetic phase transitions of the first kind in ferromagnetic $(La_{1-x}Ca_xMnO_3)$ lanthanum manganite is studied. It has been found that the stratification occurs due to a negative mode-mode interaction in the spin system, which is a necessary condition for the first-order phase transition in the Ginzburg-Landau theory. It is shown that due to the peculiarities of the electronic structure during phase separation, metal droplets possess scalar spin chirality. This leads to *sd*-scattering by spin inhomogeneities, which causes the Anderson metal-semiconductor transition near the Curie temperature and the appearance of the chiral Hall effect.

Keywords: first-order phase transition, spin density fluctuations, phase separation, Andersen localization, spin chirality, Hall effect.

DOI: 10.61011/PSS.2025.08.62267.181-25

1. Introduction

It is already known for a long time that ferromagnetic lanthanum manganites and other magnetic semiconductors with colossal magnetoresistance (CMR) are characterized by anomalous binding of spin and electron subsystems (see, for example, the reviews [1,2] and references therein). At the same time, it is found that an area of ferromagnetic long-range order is generated due to Zener double *sd*-exchange, which results in a correlation effect of reduction of the system's full energy due to motion of free *s*(*p*)-carriers with a spin that is parallel to spins of *d*-electrons of the magnetic ion. However, during magnetic first-order phase transitions effective magnetic fields related to the double exchange disappear and electron phases are separated to result in CMR [1].

The experiment indicates that phase separation is caused by crossover of the magnetic first-order phase transition and an Andersen metal-semiconductor electronic transition, which results in formation of a semiconductor matrix with metal spin droplets [1]. However, a microscopic nature of observed phase separation and, therefore, crossover of the magnetic and electronic transitions requires further research. This especially relates to still unclarified mechanisms of formation of local magnetization [3] as well as an unordinary anomalous Hall effect observed in ferromagnetic lanthanum manganites [4,5].

The study [6] has developed a band model of ferromagnetism of lanthanum manganites, which along with the double exchange effect investigated a role of Hubbard correlations that a main cause of ferromagnetic ordering in the transition metals. At the same time, indications

have been obtained that the double exchange has a decisive effect on formation of the ferromagnetic long-range order of lanthanum manganites, while in the area of phase separation, which is observed above the Curie temperature (T_C), along with strong *sd*-scattering, the Hubbard correlations start playing an important role.

However, assumptions and estimates that are made within the framework of the ferromagnetism band model are undersubstantiated. Largely, it is due to the fact that specific features of the energy electron spectrum and a fine structure of the density of electron states (DOS) of ferromagnetic lanthanum manganites as well as other ferromagnetic semiconductors with CMR are still unspecified (see, for example, the study [7,8]). Therefore, parameters of the Ginzburg-Landau functional, which determine a criterion of origination of the first- and second-order transitions [9], are not determined. In particular, it concerns a parameter of inter-mode coupling, which during the first-order transition shall change its sign from positive to negative according to the Ginzburg-Landau functional [9].

Based on *ab initio* performed simulation of an electronic structure without spin polarization, the present study considers phase separation in $La_{1-x}Ca_xMnO_3$. Using the example of $La_{0.7}Ca_{0.3}MnO_3$, it is found that during the magnetic first-order phase transition phase separation is caused by a negative inter-mode coupling and Berry curvature, which result in the chiral Hall effect.

2. Simulation of the electronic structure

The study [10] has previously simulated the electronic structure of $La_{1-x}Ca_xMnO_3$ within the framework of a

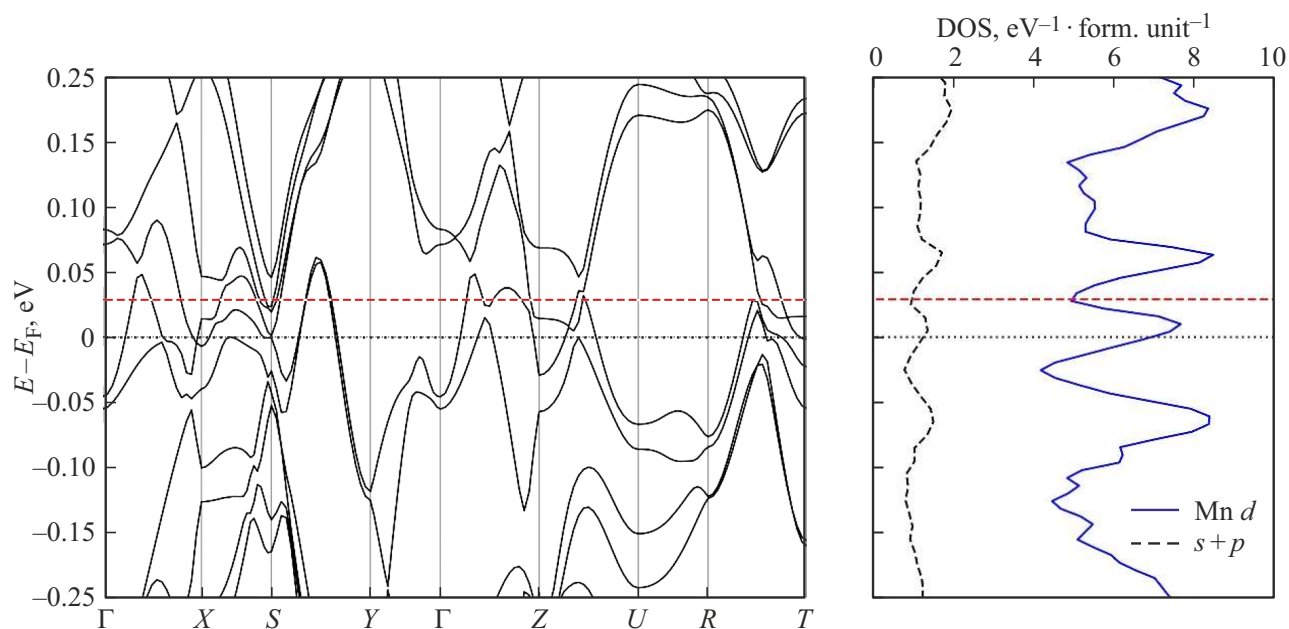


Figure 1. Density of the electron states of and the energy spectrum of $\text{La}_{1-x}\text{Ca}_x\text{MnO}_3$ near the Fermi level. The dotted line marks the Fermi level that corresponds to $x = 0.25$ (directly from DFT-calculation), while the dashed line marks the Fermi level that corresponds to $x = 0.30$.

local density approximation (LDA). At that, it used a crystal structure of cubic perovskite, which does not agree with experimental data of the study [11], according to which the considered crystal systems have an orthorhombic structure with a space group № 62, which is the same as for undoped LaMnO_3 . That is why the electronic structure of the ground state of $\text{La}_{1-x}\text{Ca}_x\text{MnO}_3$ was simulated in the present study with taking into account the orthorhombic crystal structure and within the framework of more accurate approximation for the electron density functional GGA PBE [12].

Our *ab initio* simulation included consideration of the electronic structure of the spin-nonpolarized ground state that corresponded to the area of phase separation that occurs in a paramagnetic area. It allowed considering a correlation between high-symmetry points of the electron spectrum, near which the Berry curvature occurs [13] and the fine structure of the density of electron states that determine a sign of the inter-mode coupling parameter.

The electronic structure was simulated in the Quantum Espresso software package [14] using an electron-ion interaction pseudopotential based on the projector augmented wave method (PAW). Energy of truncation of plane waves for the wave functions and the charge density/functional was 100 and 400 Ry, respectively.

The *ab initio* calculations were initially performed for $\text{La}_{0.75}\text{Ca}_{0.25}\text{MnO}_3$ by replacing one of the four lanthanum atoms with one calcium atom in the unit cell of LaMnO_3 . In order to transfer to the composition of the most studied ferromagnetic semiconductor $\text{La}_{0.7}\text{Ca}_{0.3}\text{MnO}_3$, we used a rigid band approximation, within which the Fermi level was slightly energetically shifted relative to a value

for $\text{La}_{0.75}\text{Ca}_{0.25}\text{MnO}_3$ according to the electrical neutrality condition.

Figure 1 shows results of calculation of the energy spectrum and the density of electron states (DOS) of $\text{La}_{1-x}\text{Ca}_x\text{MnO}_3$ near the Fermi level, while Figure 2 shows partial densities of electron states within a wider energy interval that comprises a band gap.

It is clear from graphs in Figures 1 and 2 that the area of transition from the composition $\text{La}_{0.75}\text{Ca}_{0.25}\text{MnO}_3$ (in which the magnetic second-order phase transition occurs) to $\text{La}_{0.70}\text{Ca}_{0.30}\text{MnO}_3$ (with the first-order transition [1]) includes an alternation of a curvature sign of the dependence

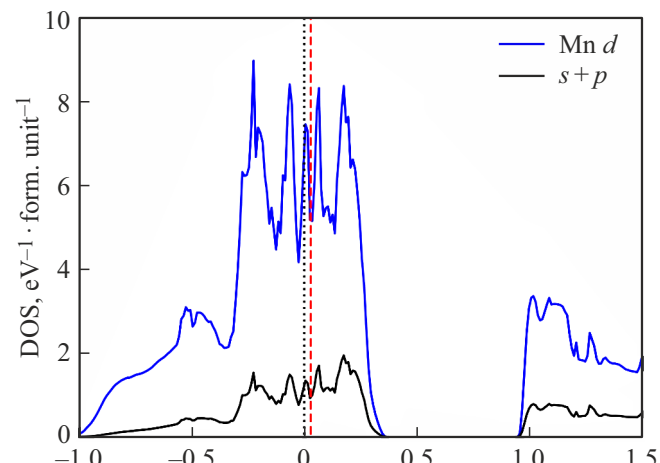


Figure 2. Partial density of electron states of $\text{La}_{1-x}\text{Ca}_x\text{MnO}_3$ (the Fermi levels are designated in the same way as in Figure 1).

of the density of states of d -electrons on the energy ($g(\varepsilon)$) near the Fermi level that is within a Berry degeneracy area.

Taking into account the Berry phases and the fine structure of the density of the electron states makes it possible to formulate a model of the first-order phase transitions in the considered ferromagnetic lanthanum manganites.

3. Model of separate of the electron phases above T_C

Investigation of phase separation that occurs in the first-order transition requires consideration of the microscopic model of the spin system with taking into account the specific features of the electronic structure, which are found in Section 2.

When investigating a ferromagnetism area in the study [6], we were based on the band model of the double sd -exchange, which took into account the Hubbard correlations of d -electrons. It was shown in good agreement with the experiment that formation of ferromagnetism of lanthanum manganites was decisively affected by the double sd -exchange, which was considered in a mean field approximation within the band model being developed.

The present study uses a generalized Hubbard Hamiltonian

$$H = \sum_{l=3,p,d} H_0^{(l)} + H_{dd} + H_{sd}, \quad (1)$$

in which a double exchange summand (H_{sd}) that is written in the mean field approximation

$$H_{sd} = -J_{sd} \sum_v \mathbf{S}_v \mathbf{s}_v \approx -J_{sd} \sum_v (\langle \mathbf{S}_v \rangle \mathbf{s}_v + \mathbf{S}_v \langle \mathbf{s}_v \rangle),$$

is supplemented by taking into account band motion of $s(p)$ - and d -electrons — $H_0^{(l)}$ and by an interatomic repulsion Hamiltonian $H_{dd} = -J_{dd} \sum_v (S_v^2 - \frac{n_v^2}{4})$, \mathbf{S}_v and \mathbf{s}_v are vector operators of the spin of d - and $s(p)$ -electron, n_v — the operator of the charge density of d -electrons in the site v .

At the same time, it can be shown that sd -scattering of electric current carriers can not be neglected within a range of the temperatures above T_C , where spontaneous magnetization resulting in the effective fields $I_{sd} \langle \mathbf{S}_v \rangle$ (see the formula (8) below and the study [6]).

Writing of an expression of the partition function of the paramagnetic state for H_{dd} with summands that are quadratic by operators of the spin and charge density included Stratonovich-Hubbard transformations that result in a picture of electron motion in fluctuating ξ - and η -fields [15]

$$\exp(-|A|^2) = \int d\zeta \cdot \exp(-|\zeta|^2 + \mathbf{A} \cdot \zeta), \quad (2)$$

where ($\zeta = \xi, \eta, A = \mathbf{S}_v, n_v$).

After these transformations, the partition function of a system of the collectivized d -electrons in an external magnetic field of strength H is written as follows:

$$Z = Z_0 \int (d\xi d\eta) \exp(-\Phi(\xi, \eta)), \quad (3)$$

Here

$$(d\xi d\eta) = d\xi_0 d\eta_0 \left[\prod_{q \neq 0, j} d\xi_q^{(l)} d\eta_q^{(l)} \right],$$

Z_0 — the partition function of d -electrons with the energy spectrum obtained during the ab initio GGA-simulation (see Figure 1), j — the index of a real ($=1$) and an imaginary ($=2$) part of the ξ - and η -fields, $q = (q, \omega_{2n})$, q — the quasi-momentum, ω_{2n} — the Matsubara Bose-frequency, while a functional of electrons in the fluctuating exchange and charge fields

$$\begin{aligned} \Phi(\xi, \eta) = & \sum_q \left[(1 + \chi_q^{(0)}) |\eta_q|^2 \right. \\ & + D_q^{(0)-1} |\xi_q - 2c^{-1} (H \delta_{q,0})|^2 \left. \right] + (4!)^{-1} \sum_q \delta_{\sum_{i=1}^4 q_i, 0} \kappa(\mu) \\ & \times \left(\xi_{q_1} \xi_{q_2} \xi_{q_3} \xi_{q_4} - \frac{3!}{2!2!} \xi_{q_1} \xi_{q_{2,m}} \eta_{q_3} \eta_{q_4} + \eta_{q_1} \eta_{q_2} \eta_{q_3} \eta_{q_4} \right) \end{aligned} \quad (4)$$

as well as the Ginzburg-Landau functional (with expansion in order parameters powers) has, along with second-order summands with the Lindhard function $\chi_q^{(0)}$ and the Stoner factor $D_q^{(0)} = (1 - U \chi_q^{(0)})^{-1}$, fourth-order summands with a mode-mode parameter

$$\kappa(\mu) = 4^{-1} J_{dd}^3 \left(\frac{g^{(2)}(\mu) - (g^{(1)}(\mu))^2}{g(\mu)} \right), \quad (5)$$

which are determined via the density of d -electron states g (Figures 1, 2) and its derivatives $g^{(1)}$ and $g^{(2)}$ when $\varepsilon = \mu$ (ν — the chemical potential of the entire system of electrons), $c = (J_{dd} T)^{1/2}$.

Evaluation of functional integrals in the expression of the partition function (3) used a procedure of saddle point by the static charge ($\eta_q^{(f)}$) and exchange ($\xi_q^{(\gamma)}$) (γ is an index of the coordinate axes) fields as well as by a modulus of the dynamic exchange fields $r_q^{(\gamma)} = |\xi_q^{(\gamma)}|$, $\xi_q^{(\gamma)} = |\xi_q^{(\gamma)}| \exp(\phi_{q,\gamma})$ (see the study [14]):

$$\partial Z / \partial \xi_q^{(\gamma)} = 0, \quad \partial Z / \partial \eta_q^{(j)} = 0, \quad \partial Z / \partial r_q^{(\gamma)} = 0$$

and took into account a relation of the exchange fields to the averages of the spin density operators [15].

At the same time, according to the saddle-point conditions, it is obtained for the area of the negative inter-mode coupling ($\kappa < 0$) that nonzero values of magnetization in the sites

$$M_{v,\gamma}^{(d)} = \sum_q M_s \exp(i q v + i \varphi_{q,\gamma}) \quad (6)$$

occur only at fixed values of the phases $\varphi_{q,\gamma}$, which coincide with differences of the electronic Berry phases (see Section 2). The modulus of local magnetization is determined as a root-mean-square value of an amplitude of static fluctuations $M_s = \langle \delta M^2 \rangle^{1/2}$, for which we have

$$\begin{aligned} \langle \delta M \rangle^2 &= N_0^{-1} \sum_v \langle (S_v - \langle S_v \rangle)^2 \rangle \\ &= \langle \delta \eta^2 / 4 \rangle - \kappa^{-1} \left[D_0^{(0)-1} + \kappa (M^2 + 5 \langle m^2 \rangle / 3) \right], \end{aligned} \quad (6a)$$

$$\begin{aligned}\langle \delta\eta^2/4 \rangle &= N_0^{-1} \Sigma_v \langle (n_v - \langle n_v \rangle)^2 \rangle \\ &= \langle \delta M^2 \rangle - \kappa^{-1} \left[2 - D_0^{(0)^{-1}} - \kappa(M^2 + 5\langle m^2 \rangle/3) \right],\end{aligned}\quad (6b)$$

where M — magnetization.

After analytically extending $D_q^{(0)}$ and $\chi_q^{(0)}$ to the real-part axis and using the Lindhard model $\chi_{q,\omega}^{(0)} = \chi_{0,0}^{(0)} + Aq^2 + iC(\omega/|q|)$, we also find a pair correlator $\langle S_\nu S_\mu \rangle \sim \langle \delta M^2 \rangle \left(\exp(-\frac{r}{R_C})/r \right)$ that reflects origination of the spin droplets in the system of d -electrons with the correlation radius $R_C \sim (AJ_{dd}\chi)^{1/2}$.

Here, paramagnetic susceptibility

$$\chi = 2\chi_0^{(0)} \left(D_1^{-1} + \kappa(2M^2 + \langle \delta M^2 \rangle + 5\langle m^2 \rangle/3) \right)^{-1}$$

sharply increases when approaching the Curie point from the paramagnetic area. At the same time, according to the fluctuation-dissipation theorem (which coincides with the saddle-point conditions for $r_q^{(y)}$) the average square of the amplitude of the thermodynamic fluctuations

$$\langle m^2 \rangle = B \left(\frac{T}{J_{dd}} \right)^2 \left(|\kappa|(M^2(H) - \langle \delta\eta^2 \rangle + \langle \delta M^2 \rangle) - A \right)^{-2} \quad (7)$$

within the area of phase separation turns out to be in $(J_{dd}/T)^2$ times less than $\langle \delta M^2 \rangle$.

Besides, considering scattering of the electric current $s(p)$ -carriers on strong spatial inhomogeneities of distribution of the electron density (6), we find that the area of phase separation exhibits origination of crossover of the magnetic first-order phase transition with the Andersen metal-semiconductor electronic transition [16].

At the same time, according to the study [6], there is a percolation threshold $E_C \sim J_{dd}\langle \delta M^2 \rangle$ forming in the system of $s(p)$ -electrons, whose intersection by the chemical potential results in hopping conductivity. As a result of this, just above the Curie temperature, electrical conductivity starts changing with the temperature as per the exponential law:

$$\sigma(T) = \sigma_0 \exp(-E_A/T), \quad (8)$$

where $E_A = (E_C - \varepsilon_c + \mu)$ — the energy of activation, ε_c — the energy of a top edge of the partly occupied d -band (Figure 2).

In order to determine temperature boundaries of the area of phase separation $T_c < T < T_s$, it is necessary to consider a temperature dependence of the chemical potential, which will determine conditions of origination of the negative inter-mode coupling with the parameter (5). This dependence can be found from the electrical neutrality requirement for the total concentration of s -, p - and d -electrons

$$\begin{aligned}n &= 2 \int d\varepsilon n(g_{s,p}(\varepsilon) + g(\varepsilon)) f(\varepsilon - \mu) \\ &\quad - 2U^2 g^{(1)} [\langle \delta M^2 \rangle + \langle m^2 \rangle - \langle \eta^2 \rangle/4].\end{aligned}\quad (9)$$

4. Hall effect in the area of phase separation

According to the developed model of phase separation, a direct consequence of the spatial inhomogeneities of distribution of the spin density (6) and the specific features of the electronic structure (Section 2) is origination of scalar spin chirality that is determined by the chiral charge χ_c (see the study [17]). In case of the ferromagnetic spin droplets

$$\chi_c = \Sigma_{v_1, v_2, v_3} \langle \mathbf{S}_{v_1} [\mathbf{S}_{v_2} \times \mathbf{S}_{v_3}] \rangle = \pm M(\langle \delta M^2 \rangle), \quad (10)$$

where $M = \chi H$.

At the same time, by taking into account the relation of local magnetization (6) to the Berry phases, it can be assumed that when traversing a circuit of sites that are related to any three different spin droplets of the radius R_C there is progression of the phases of local magnetizations. This specific feature is equivalent to what is happening when switching on the magnetic field resulting in a Hall deviation [4,17,18]. Therefore, by following the study [4], in the considered case of thermodynamically unstable ferromagnetism, at which phase separation occurs, it is possible to introduce a fictitious field (the insert in Figure 3) that is perpendicular to a plane of the planar sample and results in the Hall deviation

$$\mathbf{b} = \pm \Sigma_{v_1, v_2, v_3} \langle \mathbf{S}_{v_1} [\mathbf{S}_{v_2} \times \mathbf{S}_{v_3}] \mathbf{n}_{v_1, v_2, v_3} \rangle,$$

where $\mathbf{n}_{v_1, v_2, v_3}$ is a unit vector that is perpendicular to the plane of a triangle constructed at the sites.

As a result of this, we have the situation when resultant phase separation leads to a chiral contribution to the Hall resistance, which, in the same way as the contribution by the anomalous Hall effect, is approximately proportional to magnetization

$$\rho_{xy} = R_0 \chi_c = R_s M, \quad (12)$$

but with the Hall constant

$$R_s = R_0 \exp(T^{-1}E_A) \langle \delta M^2 \rangle, \quad (13)$$

which is related to scalar spin chirality that is proportional to the normal effect constant (R_0).

Figure 3 compares the calculated temperature dependence of the Hall constant R_s with the experimental data for $\text{La}_{0.7}\text{Ca}_{0.3}\text{MnO}_3$ [5]. It is shown at the same time that a metal ferromagnetic area exhibits its sharp increase with the temperature, which is related to thermodynamic spin fluctuations (7). Above the Curie temperature, phase separation occurs, at which the thermodynamic spin fluctuations are suppressed, thereby resulting in the temperature dependence of the Hall constant (13), which is related not only to the metal-semiconductor transition, but an effect of origination of spin chirality.

When calculating the dependence $R_s(T)$, we used interaction parameters of the study [6] $J_{dd} = 1.2$ and $J_{sd} = 0.6$ eV, parameters of the Lindhard function $A = 0.07$ and $C = 1.28$, which are obtained in an effective mass

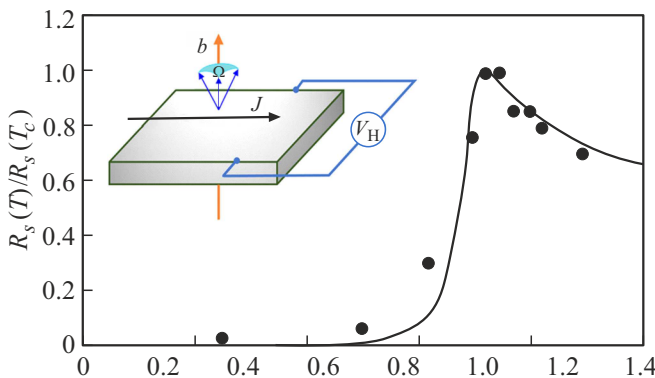


Figure 3. Temperature dependence of the parameters of the anomalous and topological Hall effects for $\text{La}_{0.7}\text{Ca}_{0.3}\text{MnO}_3$. The solid line marks a calculation, while the dots mark experimental data [5]. The insert schematically shows a mechanisms that results in origination of the chiral Hall effect (borrowed from the study [4]), where J is the current value.

approximation, as well as results of calculation of the electronic structure, which are given in Section 2. At the same time, for the area of phase separation $T_c < T < T_s$, we obtained the values $T_c = 220$ and $T_s = 310$ K, whereas according to processing of the experiment [4,5], which was performed on the planar samples of the thickness of 150 nm, they are just 250 and 350 K, respectively.

When $T > T_s$, according to (9), there is a temperature shift of the chemical potential beyond the Berry curvature energy area, resulting in disappearance of spin chirality.

5. Conclusion

Thus, we see from the results of the *ab initio* simulation of the electronic structure that due to the fine structure of the density of the electron states during the magnetic first-order phase transition ferromagnetic lanthanum manganites exhibit the negative inter-mode coupling and the Berry curvature. It is shown that it results in formation of the area of electron-phase separation, which consists of the semiconductor matrix of $s(p)$ -electrons and metal droplets of d -electrons with scalar spin chirality that are „immersed“ therein.

At the same time it is shown that within the temperature range of phase separation ($T_c < T < T_s$) the chiral Hall effect is formed.

We see from analysis of the obtained results that the slight energy concentration shift of the chemical potential relative to the area of negative curvature of the density of the electron states (Figure 1) can result in the fundamental change of the spintronic properties of $\text{La}_{1-x}\text{Ca}_x\text{MnO}_3$ (for example, for the compositions with the calcium doping concentrations from $x_1 = 0.25$ to $x_2 = 0.30$).

At the same time, it is interesting to further investigate doping of manganite $\text{La}_{0.75}\text{Ca}_{0.25}\text{MnO}_3$ (that is in tricritical state) with calcium impurities. It would allow not only

refining boundaries of the range of the compositions with the first-order phase transition, but studying an interrelation of origination of CMR and the chiral Hall effect as well.

Further (first of all, experimental) research of the spintronic properties within the area of phase separation of ferromagnetic lanthanum manganites is believed to be important when designing spin-current oscillators.

Funding

The results were obtained as part of the assignment of the Ministry of Science and Higher Education, contract No. FEUZ-2023-0015.

Conflict of interest

The authors declare that they have no conflict of interest.

References

- [1] N.G. Bebenin, R.I. Zainullina, V.V. Ustinov. UFN **188**, 8, 801 (2018). (in Russian).
- [2] Yu.A. Izyumov, Yu.N. Skryabin. UFN **171**, 2, 121 (2001). (in Russian).
- [3] D. Pchelina, V. Sedykh, N. Chistyakova, V. Rusakov, Y. Alekhina, A. Tselebrovskiy, B. Fraisse, L. Stievano, M.T. Sougrati. J. Phys. Chem. Sol. **159**, 110268 (2021).
- [4] H. Wang, Y. Dai, G.-M. Chow, J. Che. Prog. Mater. Sci. **130**, 100971 (2022).
- [5] P. Matl, N.P. Ong, Y.F. Yan, Y.Q. Li, D. Studebaker, T. Baum, G. Dabinina. Phys. Rev. B **57**, 10248 (1998).
- [6] A.A. Povzner, A.G. Volkov, E.I. Lopatko, N.A. Zaitseva. FTT **65**, 4, 545 (2023). (in Russian).
- [7] Topological Magnetic Materials Database: <https://www.topologicalquantumchemistry.fr/magnetic>.
- [8] Topological Materials Database: <https://topologicalquantumchemistry.com>.
- [9] M. Brando, D. Belitz, F.M. Grosche, T.R. Kirkpatrick. Rev. Mod. Phys. **88**, 25006 (2016).
- [10] W.E. Pickett, D.J. Singh. Phys. Rev. B **53**, 3, 1147 (1996).
- [11] W. Tang, W. Lu, X. Luo, B. Wang, X.B. Zhu, W. Song, Z. Yang, Y. Sun. J. Magn. Magn. Mater. **322**, 2360 (2010).
- [12] J. Perdew, K. Burke, M. Ernzerhof. Phys. Rev. Lett. **77**, 3865 (1996).
- [13] M.A. Wilde, M. Dodenhoff, A. Niedermayr, A. Bauer, M.M. Hirschmann, K. Alpin, A.P. Schnyder, C. Pfleiderer. Nature **594**, 374 (2021).
- [14] P. Giannozzi, O. Andreussi, T. Brumme et al. J. Phys.: Condens. Matter **29**, 465901 (2017).
- [15] T. Moriya. Spinovye fluktuatsii v magnetikakh s kollektivizirovannymi elektronami. Mir, M. (1988). 288 s. (in Russian).
- [16] F. Anderson. UFN **127**, 1, 19 (1979). (in Russian).
- [17] K.S. Denisov, I.V. Rozhansky, N.S. Averkiev, E. Lähderanta. Phys. Rev. Lett. **117**, 027202 (2016).
- [18] A.F. Barabanov, Yu.M. Kagan, L.A. Maksimov, A.V. Mikheenko, T.V. Khabarova. UFN **185**, 5, 479 (2015). (in Russian).

Translated by M.Shevlev